*Desalination and Water Treatment*
www.deswater.com

doi:10.5004/dwt.2018.22346

114 (2018) 109–119
May

# Groundwater share quantification through flood hydrographs simulation using two temporal rainfall distributions

Khaled S. Balkhair[a,b,*], Amjad Masood[a,c], Mansour Almazroui[d], Khalil Ur Rahman[a,e], Omar A. Bamaga[b], Ahmed S. Kamis[a], Iqbal Ahmed[b], Mohammed I. Al-Zahrani[f], K. Hesham[g]

[a]*Department of Hydrology and Water Resources Management, King Abdulaziz University, Jeddah, Saudi Arabia, email: kbalkhair@kau.edu.sa (K.S. Balkhair)*
[b]*Center of Excellence in Desalination Technology, King Abdulaziz University, Jeddah, Saudi Arabia*
[c]*Global Change Impact Studies Centre, Islamabad, Pakistan*
[d]*Center of Excellence for Climate Change Research/Department of Meteorology, King Abdulaziz University, Jeddah, Saudi Arabia*
[e]*Department of Hydraulic Engineering, Tsinghua University, Beijing, China*
[f]*Saudi Geological Survey, Jeddah, Saudi Arabia*
[g]*Department of Geophysics, King Abdulaziz University, Jeddah, Saudi Arabia*

Received 7 November 2017; Accepted 4 February 2018

**ABSTRACT**

Due to the scarcity, randomness, and extremity of rainfall events in arid regions, planning and management of water resources are essential. Rainfall in many arid regions such as Saudi Arabia is characterized by high intensity and short duration during which flash floods occur and cause not only major loss in life and structures but also a huge loss of clean water. Understanding the relationship between rainfall and runoff is the key issue in the management and control of water resources. In this study, two approaches have been applied using Hydrologic Engineering Center's Hydraulic Modeling System model to simulate flood hydrographs of a mountainous watershed located on the west side of Saudi Arabia. The first approach was based on incorporating losses through the soil conservation service (SCS) curve number and SCS unit hydrograph. The second approach was based on effective rainfall in which excess rainfall was computed by Horton's infiltration method and the Phi index method. Results revealed that the performance of losses incorporation approach was poor in simulating runoff hydrographs in all studied storms. Its main drawback was the ineffective representation of flow mass conservation and the early generation of runoff due to rainfall input. In contrast, the effective rainfall approach simulated runoff hydrographs efficiently; moreover, results were comparable with many of those reported in the literature. The two critical hydrograph parameters of peak flow and time to peak were simulated accurately by Phi index method and Horton's infiltration method. The sensitivity analysis showed that the peak flow is directly proportional to the curve number and inversely proportional to the initial abstraction. From water management point of view, the simulated hydrographs added a valuable piece of information about the quantification of lost and stored rainwater. About 55%–70% of rainwater infiltrates through the soil profile and recharges the underlined groundwater reservoir, hence becomes a major source of water in the region.

*Keywords:* Arid regions; Excess rainfall; Floods hydrograph; Temporal distribution; HEC-HMS; Clean water

* Corresponding author.

1944-3994/1944-3986 © 2018 The Author(s). Published by Desalination Publications.

## 1. Introduction

With low annual rainfall rate, high temperature, and no rivers or water bodies, Saudi Arabia with the exception of the southwestern region is classified as an arid region. Therefore, the country is considered among the poorest countries in the world in terms of naturally renewable water resources. Although, the number of rainy days per year in many regions of Saudi Arabia is very few, however, rainfall events are characterized by high intensity and short duration, causing flash floods and loss of huge quantities of good quality water. Therefore, the development of a decision support system in these regions is required to fortify flash flood and water resource management [1].

The first step in developing a decision support system is to understand the relationship between rainfall and runoff processes. This relationship has been studied for decades [2–8]. In some studies, the morphometric characteristics of basins have been used to foresee and illustrate flood peaks and estimation of erosion rate [9]. Patton [10] has explained how the application of geomorphologic principles to flood potential or flood risk has led to a significant amount of research to identify the interactions between basin morphometric and flooding impact [10–13]. Flood hydrographs are considerably affected by the temporal and spatial distribution of rainfall [14]. Rainfall is one of the main hydrological factors influencing the magnitude and shape of the associated runoff hydrograph during a flood event. Its temporal and spatial variations contribute significantly to the hydrograph time to peak, peak discharge, and flood volume.

The event basis analysis consists of separating rainfall events, identifying representative events of different magnitudes, determining the origin of characteristics parameters, and interpreting statistics [5]. However, in one particular study carried out by Abustan et al. [15], the authors focused on discovering the amount of runoff generated by different storm events. The authors randomly selected a total of 90 storm events over a 6-year period (1998–2003) throughout the catchment. The event analysis involved constructing the hydrographs and hyetographs to determine the relationship between the amount of rainfall and volume of runoff generated during the storm [15]. Bournaski et al. [16] investigated the relationship between rainfall–runoff in Dernah area, Al Jabal Al Akhdar, NE Libya. His model examined the morphometric parameters of four wadis in which an integration analysis has been carried out between morphometric parameters and geographic information system (GIS) techniques.

Water resources in Saudi Arabia are mostly derived from groundwater (originated from rainfall) and occasional surface runoff where water management projects are applied [17]. The annual rainfall depth in some regions is as low as 50 mm; however, due to rainfall characteristics, destructive floods may occur. For example, two extreme catastrophic floods hit Jeddah city in 2009 and 2011 leaving behind loss in life and destruction to buildings and structures. Studying these rainfall characteristics and the relationship between rainfall and runoff in such regions is essential and mandatory for flood protection, rainwater harvesting projects, and water resources management in general. Wadis, a synonym of valleys, consist of sub-catchments which usually receive rain at the sides of mountains. This rainwater accumulates and flows in different tributaries that are connected to a wadi's mainstream. As a result, and depending on the magnitude of the event, surface water flows out of a wadi through its outlet either towards the seaside in coastal regions or inland. A few days or weeks after a rainfall event, most of the surface water in a wadi has been infiltrated and become groundwater. A typical example of such areas is Wadi Al-Lith at the western side of Saudi Arabia. To quantify resident water or outflow, several variables need to be identified including land use, soil properties, infiltration rates, initial abstraction, and hydraulic properties of the wadi streams. Computer models such as Hydrologic Engineering Center's Hydraulic Modeling System (HEC-HMS), Hydrologiska Byrans Vattenavdelning, and Water Evaluation and Planning System usually take into consideration these variables and more.

HEC-HMS and soil conservation service (SCS) are widely used in different climatic zones including arid watersheds to simulate and forecast streamflow. Previous studies on HEC-HMS proved its ability to simulate and forecast streamflow based on different datasets and catchment types [8,16,18,19]. Abushandi and Merkel [20] applied HEC-HMS to simulate a single streamflow event in Wadi Dhuliel arid catchment. They concluded that the calibration of the model was an essential step to reduce prediction errors for a single storm event. Du et al. [21] used HEC-HMS to examine effects of urbanization on annual runoff and flood events of the Qinhuai River watershed in Jiangsu Province, China. Shadeed and Almasri [22] demonstrate that the integration of GIS with the soil conservation service curve number (SCS-CN) method provides a powerful tool for estimating runoff volumes in West Bank catchments, representing arid to semi-arid catchments of Palestine. Estimated and observed runoff depths of four examined events were close enough to assume the applicability of the GIS-based SCS-CN approach for the region. Radmanesh et al. [23] calibrated and validated the HEC-HMS model in Yellow River watershed in southwestern Iran. Their results showed a good fit between the peak discharge of observed and simulated hydrographs. Kafle et al. [24] have studied the effect of rainfall on runoff generation in Bagmaty basin (Vietnam) with HEC-HMS model. Their results were similar to those found by Radmanesh et al. [23]. Credible results were obtained by Al-Ahmadi [25] in the application of HEC-HMS, GIS, and remote sensing by automated calibration method in three sub-basins in the southwestern region of Saudi Arabia.

This study examines the relationship between rainfall and runoff hydrograph of an arid wadi through two different representations of rainfall events. Commonly used temporal rainfall distributions are SCS and Huff distributions. These distributions are mainly derived and frequently applied to humid environments which differ from arid areas. It is assumed that the applications of such distributions to arid land hydrological events may cause some discrepancies. However, these two distributions are used in modeling hydrographs by watershed modeling system and HEC-HMS models. Due to abnormal rainfall–runoff characteristics in arid regions, the resulting hydrographs will be compared with observed hydrographs to calibrate and examine the proposed distributions. A temporal distribution that causes higher peaks and/or critical cases must be defined. Such a study will be important for best applications of hydrological models in the ungauged catchment in arid environments. This study deals with rainfall–runoff analysis using HEC-HMS model. The objective is to establish a relationship between rainfall and flood hydrographs of Wadi Al-Lith through simulation with HEC-HMS with SCS-CN method under two different temporal rainfall distributions. Consequently, the simulated hydrographs quantify the lost and stored rainwater in the studied wadi.

## 2. Materials and methods

### *2.1. Study area*

Wadi Al-Lith is located in the western part of the Kingdom of Saudi Arabia, approximately 200 km south of Jeddah city. It lies between 40°10' and 40°50' longitude and 20°00' and 21°15' latitude and comprises an area of approximately 3,262 km$^2$ (Fig. 1). Geologically, Wadi Al-Lith is underlain by late Proterozoic plutonic, metavolcanic, and metasedimentary rocks in most of the wadi comprising approximately 86.8% of the total area by chiefly tertiary sedimentary, volcanic, and plutonic rocks in and near the coastal plain, and by tertiary oceanic crust of the Red Sea offshore [26].

The study area, which is located within the Tehama escarpment of the Arabian Shield, is characterized by semi-annual flash floods. In November 2009 and December 2010, Wadi Al-Lith received two catastrophic flash floods which left many people dead and destroyed many infrastructures [27]. In this study, the upper sub-catchments which are located between 20°30' and 21°15' latitude and 40°10' and 40°50' longitude with an area of 1,710 km$^2$ are considered in the analyses. Data from two meteorological stations (J-241 and J-238) and one hydrologic station (J-417) are considered in the rainfall–runoff analysis (Fig. 1). The topography of the wadi shows that there is an acute gradient in the catchment. The elevation changes between 0 and 2,643 m just in 1° latitudinal increase (Fig. 2).

### *2.2. Input data*

The selection of rainfall and its associated runoff events was very limited in this study due to the lack of observations, specifically flood hydrographs. The Ministry of Water and Electricity which is responsible for the water sector in Saudi Arabia has no recording runoff stations in most of the wadis across the country. Although rainfall stations are distributed all over the country, the recorded rainfall events from these stations lack any associated runoff hydrographs; hence, these records are useless in verifying model results by the proposed approaches. However, between 1984 and 1988, Dames & Moore, a US company conducted a comprehensive project on water status at selected regions in Saudi Arabia. Our study area is located in one of these regions; thus, we collected the required data from the reports of Dames & Moore [28]. Accordingly, four rainfall events and their associated recorded runoff hydrographs at station J-417 were selected for application of the model. Rainfall storms and basin characteristics of four selected events are shown in Table 1. Hyetographs of these events are shown in Fig. 3.

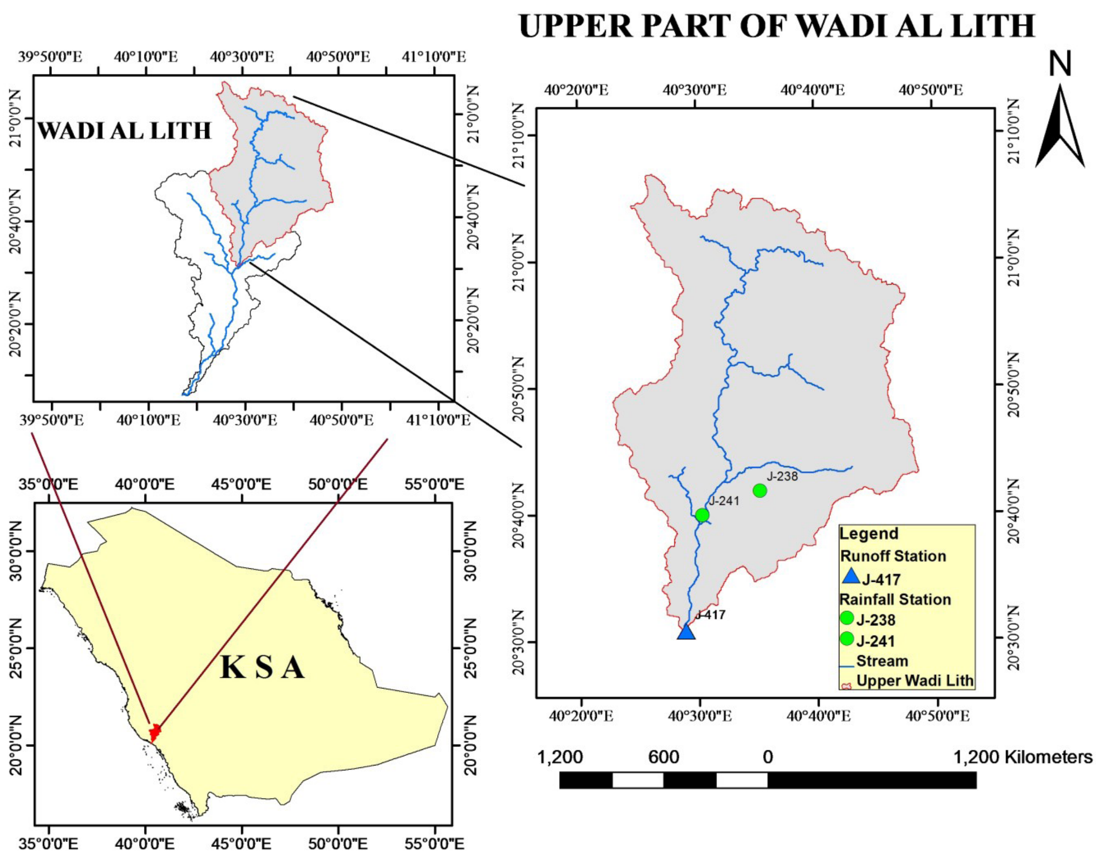


Fig. 1. Location of upper part of Wadi Al-Lith with rainfall and runoff stations indicated.

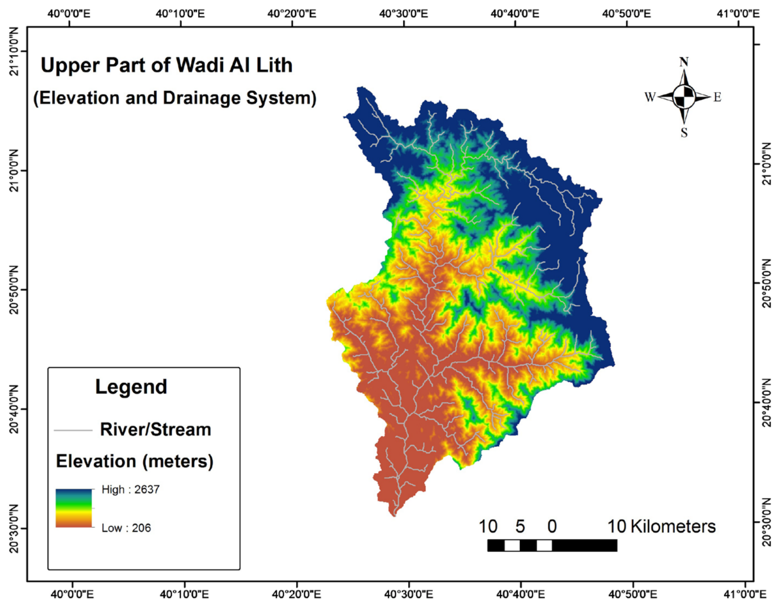


Fig. 2. Elevation and drainage system of upper part of Wadi Al-Lith.

Table 1
Storms and basin characteristics at runoff station J-417

| No. | Rainfall events | Rainfall duration (h) | Average intensity (mm/h) | Total rainfall (mm) | $I_a$ (mm) | $T_L$ (min) | CN | Imperviousness (%) | Runoff coefficients (%) |
|---|---|---|---|---|---|---|---|---|---|
| 1 | 01 Jul 1985 | 5 | 0.77 | 3.85 | 0.385 | 536 | 90 | 30 | 6.25 |
| 2 | 11 Apr 1985 | 8 | 1.87 | 14.96 | 1.496 | 413 | 90 | 30 | 1.11 |
| 3 | 17 May 1985 | 5 | 1.1 | 5.5 | 0.55 | 607.4 | 90 | 30 | 8.47 |
| 4 | 22 Apr 1985 | 7 | 1.7 | 11.9 | 1.19 | 293 | 90 | 30 | 20.90 |

### *2.3. Rainfall–runoff model*

The HEC-HMS model is a physically based, semi-distributed hydrologic model developed by the US Army Corps of Engineers to simulate the hydrologic response of a watershed subject to a given hydrometeorological input [29]. The model utilizes essential digital elevation model (DEM) information to divide the basin into sub-watersheds, and the size of the sub-watershed is determined as a priori by the modeler. The model with an input at the minute, hourly, or daily time steps can simulate individual storm events, as well as continuous precipitation. A variety of model options is available to simulate runoff production offered by the HEC-HMS. These options are comprised of SCS-CN, SCS unit hydrograph, and base flow estimation methods which are needed to calculate water losses, runoff transformation, and base flow rates. In this study, four rainfall–runoff events were selected for HEC-HMS model application. The software includes many commonly used hydrological analysis procedures such as event infiltration, unit hydrographs, and hydrologic routing. Supplemental analysis tools are provided for model optimization, forecasting streamflow, and depth-area reduction. More details are available in the technical reference manual [30]. The following two main approaches were proposed to simulate runoff hydrographs: losses incorporation approach (LIA) and excess rainfall approach (ERA). In the LIA, SCS-CN and SCS unit hydrograph methods were employed as loss and transformation methods, respectively.

### *2.4. Losses incorporation approach*

In this approach, event based hyetographs have been used to produce runoff hydrographs with SCS-CN to account

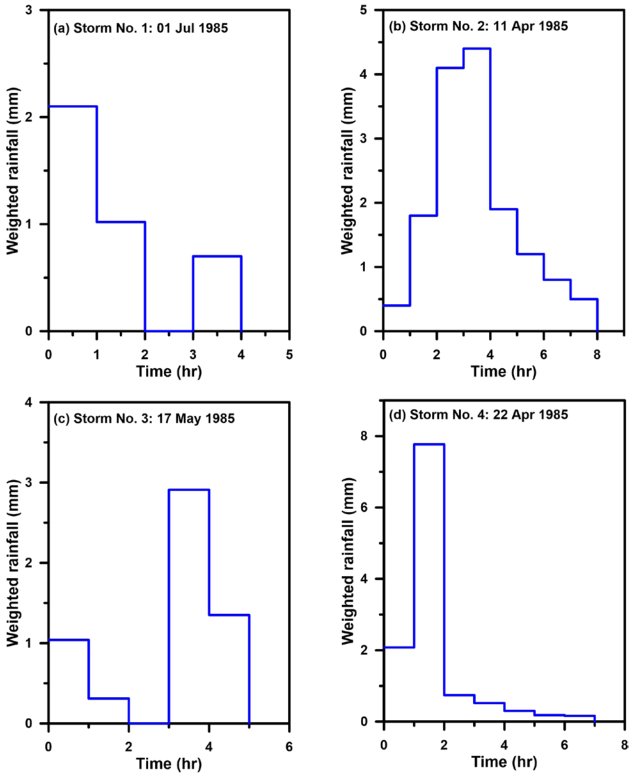


Fig. 3. Hyetographs of the selected storm events.

for losses and SCS unit hydrograph to account for transformation. Excess rainfall, as a function of cumulative precipitation, soil cover, land use, and antecedent moisture, is estimated by the SCS-CN model with the help of the following equation:

$$P_e = \begin{cases} \dfrac{(P - I_a)^2}{P - I_a + S} & P > I_a \\ 0 & P \le I_a \end{cases} \tag{1}$$

where $P_e$ is the accumulated precipitation excess at time $t$; $P$ is the accumulated rainfall depth at time $t$; $I_a$ is the initial abstraction (initial loss); and $S$ is the potential maximum retention.

Potential maximum retention is a measure of the ability of a watershed to abstract and retain storm precipitation. The precipitation excess, and hence the runoff, will be zero until the accumulated rainfall exceeds the initial abstraction.

The SCS developed an empirical connection of $I_a$ and $S$ from results obtained by numerous small experimental watersheds.

$$I_a = 0.2\ S \tag{2}$$

Therefore, the cumulative excess at time $t$ is

$$P_e = \frac{(P - 0.2S)^2}{P - 0.8S} \tag{3}$$

Incremental excess for a time interval is computed as the difference between the accumulated excess at the period's beginning and end. Through an intermediate parameter, the curve number (CN), the maximum retention, $S$, and watershed characteristics are related as

$$S = \frac{25,400 - 254\text{CN}}{\text{CN}} \tag{4}$$

CN values vary from 30 to 100. Lower numbers indicate lower runoff potential while larger numbers indicate increasing runoff potential. With the help of tables published by the SCS, the CN for a watershed can be estimated as a function of land use, soil type, and antecedent watershed moisture. Using these two tables and information of the soil type and land use, a single valued CN can be established [30].

Excess rainfall approach: Two methods of excess rainfall calculations have been employed in this approach, they are: (a) Horton's infiltration method (HIM) and (b) Phi index method (PIM).

Horton's infiltration approach: Horton's infiltration function [31] is well-established in the literature. The infiltration rate is given as a function of three parameters:

$$f_p = f_c + (f_0 - f_c)e^{-kt} \tag{5}$$

where $f_p$ is the infiltration capacity at some time $t$ (depth/time); $k$ is the constant that represents the rate of decrease in $f$ capacity; $f_c$ is the final or equilibrium capacity (depth/time); $f_0$ is the initial infiltration capacity (depth/time).

It specifies that if the rainfall supply goes beyond the infiltration capacity, infiltration tends to reduce exponentially. Though simple in form, difficulty in determining represented values for $f_0$ and $k$ confine the utilization of this equation. The area below the curve for any time interval represents the depth of water infiltrated during that interval. The infiltration rate is given by mm/h and time '$t$' in hours, and the coefficient $k$ is determined in view of that.

The area above the curve represents the rainfall excess which equals the direct runoff hydrograph. For example, in storm 22 Apr 1985, both infiltration capacity and excess rainfall are visibly below and above the infiltration curve, respectively, as shown in Fig. 4. This excess rainfall is then segregated into divisions with user-specified time intervals and made a ready input to HEC-HMS.

### 2.5. Phi index method

Infiltration indexes, in general, assume that infiltration takes place at some constant or average rate throughout a storm. Consequently, initial rates are underestimated and final rates are overestimated when a whole storm sequence with little antecedent moisture is considered [32]. The most common indexes are termed as the phi (ϕ) index for which the total volume of the storm period loss is estimated and distributed uniformly across the storm pattern. The volume of precipitation over the index line is equal to the excess rainfall (runoff). ϕ is index determined by computing the amount of observed runoff for a known storm from the hydrograph; next, the difference between this quantity and the total gauged precipitation is calculated. The volume of loss (which includes the effects of interception, depression storage, and infiltration) is distributed uniformly across the storm patterns as shown in Fig. 5. The following formula is used to calculate ϕ index:

$$R_d = \sum_{n=\oplus}^{N} \left(P_n - \Phi\Delta t\right) \tag{6}$$

where $R_d$ is the direct runoff depth; $P_n$ is the observed rainfall; ϕ is Phi index; $N$ is the number of rainfall intervals contributing to direct runoff; Δ$t$ is the time interval; and $n$ is the interval index.

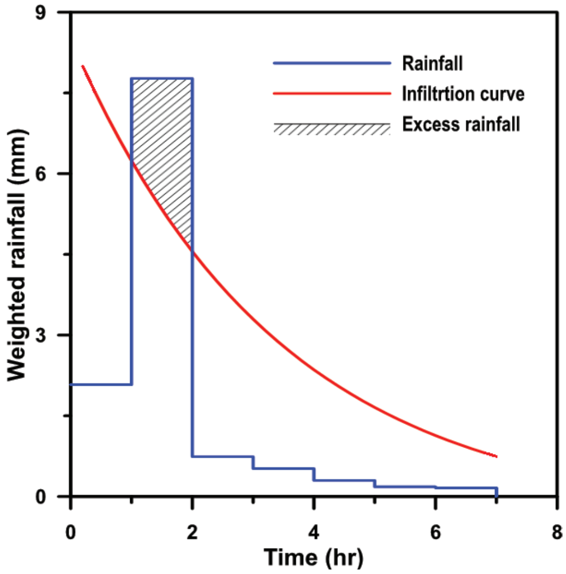


Fig. 4. Horton's infiltration curve and excess rainfall separation of the event no. 4.

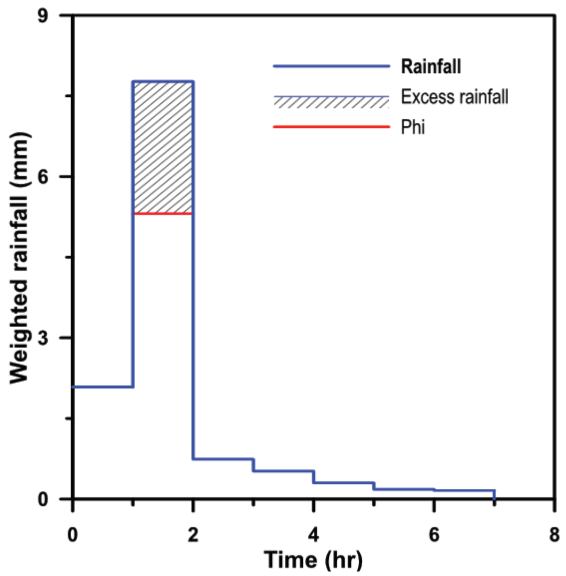


Fig. 5. Excess rainfall separation by the Phi index method.

The excess rainfall obtained by this method is then used in HEC-HMS against the corresponding time hour to produce runoff.

## 3. Results and discussion

The hyetographs of the four storms are shown in Fig. 6. The highest rainfall depth was 14.96 mm which occurred over 8 h in the storm no. 2, and the lowest rainfall depth was 3.85 mm which occurred over 5 h in the storm no. 1. Although these rainfall depths are quite low, they produced a considerable amount of runoff. The runoff coefficient, which is the quantity of excess rainfall divided by the total rainfall, is shown in Table 1 for each event. The values of runoff coefficient obtained for the selected storms range from 1.1% to 21%. This considerably wide range of values indicates high variability in the relationship between rainfall and runoff. However, many factors affect the value of runoff coefficient including rainfall characteristics and antecedent soil moisture content.

### *3.1. Losses incorporation approach*

The four input critical parameters, CN, initial abstraction ($I_a$), imperviousness, and lag time ($T_L$) in the SCS method were computed with results shown in Table 1. CN depends on land use, land cover, and antecedent moisture conditions of the basin while $I_a$ is taken as approximately 10% of the total rainfall [33]. Imperviousness, which accounts for the rocky areas of the basin, was calculated to be 30%. Fig. 6 shows the results obtained by LIA.

The figure contains four plots (a), (b), (c), and (d) with each showing observed rainfall hyetograph, observed runoff

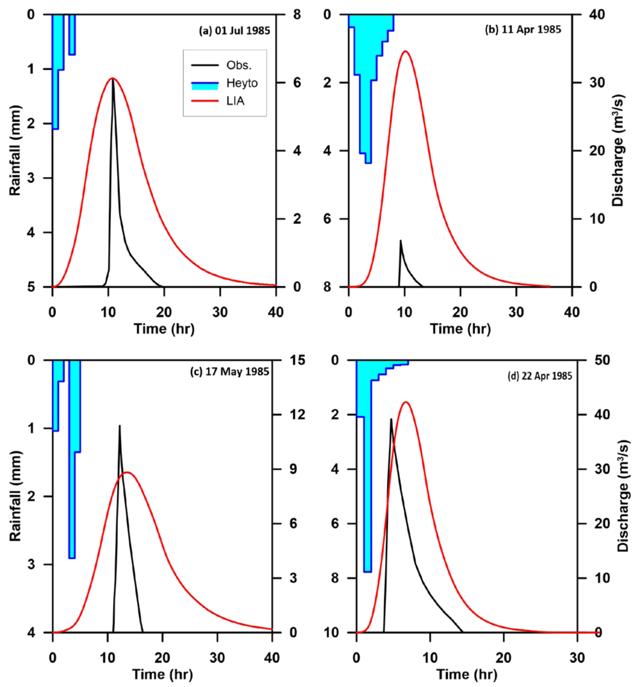


Fig. 6. LIA simulated runoff hydrographs plotted against observed hydrograph.

hydrograph, and simulated runoff hydrograph. Simulated peak flow ($Q_p$) measurements are not in a good agreement with the observed values in any storm except the storm no. 1, which shows a good match. Simulated $Q_p$ of the storm no. 3 overestimated the observed peak by 23%. The worst scenario obtained by this approach was in a storm no. 2 where the simulated $Q_p$ overestimated the observed $Q_p$ by 385%. On the other hand, time to peak ($T_p$), which is the time from the beginning of runoff to the peak flow, was overestimated by the model in all storms. This overestimation occurred because the model generated runoff right at the beginning of the rainfall event, while the observed runoff occurred immediately after the end of the rainfall event and reached its peak in a very short time. For example, in a storm no. 1, the simulated time to peak was approximately 32 times more than the observed $T_p$. This is considered a big difference and is incomparable to values published in the literature. Another overestimated parameter by this approach is the runoff volume ($Q_v$). Theoretically, volumes of simulated and observed runoffs should match, regardless of other hydrograph parameters. It is apparent that the runoff volume was overestimated in all simulated floods, which is a clear indication that the SCS-CN method poorly considers mass conservation. Another cause of overestimation and underestimation in the values of $Q_p$, $Q_v$, and $T_p$ could be the rainfall characteristics – not only intensity and duration of the rainfall event but also its temporal distribution. However, this cause has not been explored here due to lack of relevant data.

HEC-HMS accepts any increment of rainfall as input and generates the corresponding runoff hydrograph. Only hourly rainfall data were available for all selected storms. In other words, rainfall intensities were averaged over a 1-h duration. Therefore, if there were an actual variability in rainfall intensity during a 1-h duration, it would not be captured by the model. Accordingly, a bias estimation in the simulated runoff hydrographs would be expected. Due to the abovementioned causes, in addition to the uncertainty in the temporal rainfall distribution, many results of simulated hydrograph parameters found in the literature were superior to those obtained by LIA. For example, the study of [34] obtained good agreement between observed and simulated flows during HEC-HMS calibration; however, flows were underestimated during the validation process. Similarly, Reza [35] found fewer differences between observed and estimated peak and volume of flood discharge in one basin (10% and 1.2%, respectively). In another basin, Reza [35] found differences between observed and estimated peak and volume of flood discharge to be 1.48% and 3.77%, respectively. In another study, Abushandi and Merkel [20] showed that the flow comparison between the calibrated streamflow results fit well with the observed streamflow data in HEC-HMS with Nash–Sutcliffe efficiency ($E_f$) of 0.88 as compared with another hydrologic model IHACRES ($E_f$ = 0.51).

Spatial distribution of rainfall and antecedent moisture condition are two important phenomena which are not fully considered in the SCS method. Therefore, overestimation and underestimation of $Q_p$, $Q_v$, and $T_p$ were simulated. For example, storms which have maximum intensities at upstream produce late time to peak as compared with storms which occur in the middle or at the downstream side of the basin. The antecedent moisture condition may facilitate the generation of high values of peak flows in a short duration, hence resulting in low time to peak. In their study, Jin et al. [36] reported that the HEC-HMS is a suitable tool for modeling the rainfall–runoff processes; moreover, the authors noted that the SCS-CN model performed better than the initial and constant-rate model in the estimation of runoff generation.

### 3.2. Excess rainfall approach

In this approach, the following two methods were proposed to compute the effective (excess) rainfall: HIM and PIM.

#### 3.2.1. Horton's infiltration method

This approach was applied by introducing effective rainfall as obtained from HIM. The initial infiltration capacity $f_0$ and the final infiltration capacity $f_c$ were found from the experimental infiltration curve. A range of 2.30–13.0 mm/min was obtained for $f_0$ while $f_c$ was found equal to 1.5 mm/min which was taken as the average saturated hydraulic conductivity of the wadi. The constant *k*, which represents the rate of *f* decrease in Eq. (5), was fitted to the HIM and found equal to 0.293.

Infiltration capacity *f* in Horton's equation is a function of time *t*. The initial infiltration rate $f_0$, which depends solely on the antecedent moisture condition of the soil, reaches maximum values in dry soils and minimum values in moist soils. In this study, $f_0$ was taken as a function of antecedent soil moisture conditions of the soil (obtained from Dams and Moore report). Average values of $f_0$ were found as 2.30, 13.0, 5.8, and 10.40 mm/h for storm nos. 1, 2, 3, and 4, respectively.

Simulated hydrographs by this approach are shown in Fig. 7. Although $Q_v$ and $T_p$ are slightly overestimated or underestimated in most of the storms, simulated hydrographs are much better than those obtained by LIA. Simulated peak flows were found in a good agreement with the observed values in all storms. The best match was found in the storm no. 4, plot (d), where both simulated and observed values $Q_p$ were identical. In contrast, the poorest match was obtained in a storm no. 3, plot (c), where $Q_p$ was underestimated by 16.4%. A similar result was also found in a storm no. 2, plot (b). On the other hand, while $Q_v$ was overestimated in the storm no. 2 by 0.51%, it was underestimated in the rest of the storms. The worst scenario was obtained in the storm no. 3 with an underestimation of 16%. On the other hand, the simulated time to peak in all storms was much better than that obtained by LIA; however, the observed values were still underestimated.

#### 3.2.2. Phi index method

This approach was applied by introducing effective rainfall obtained by PIM. Infiltration indexes generally assume that infiltration occurs at some constant or average rate throughout a storm event. Consequently, initial rates are underestimated and final rates are overestimated when a whole storm progression with little antecedent moisture is considered. In this index, the total volume of the storm loss is estimated and distributed uniformly across the storm pattern. The resultant Phi line is plotted against the rainfall hyetographs for all storms as shown in Fig. 7. The rainfall depth

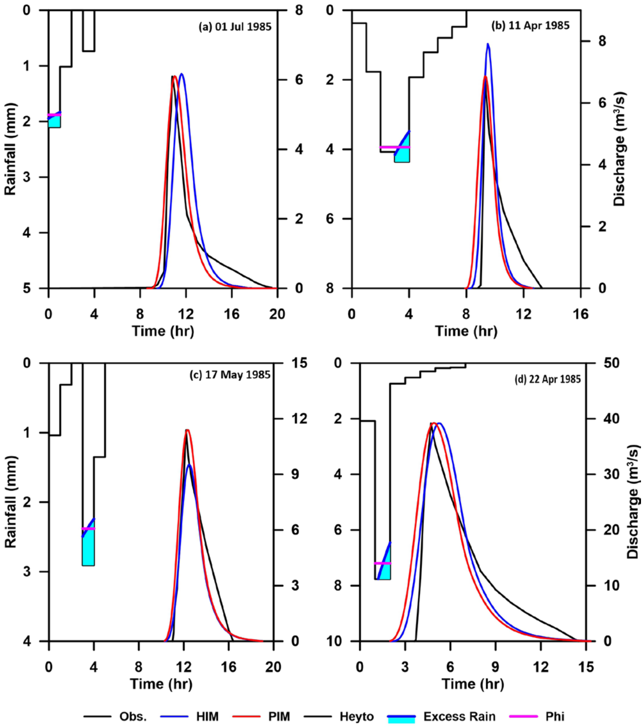


Fig. 7. Simulations runoff hydrographs by HIM and PIM plotted against observed hydrograph, the excess rainfall computed by Horton's infiltration method.

(excess rainfall) above the Phi index line is equivalent to the runoff depth; that is, the volume generated by the excess rainfall is equivalent to the observed runoff volume. The Phi value for each event was computed and the results are shown in Table 2. The wide range of Phi values (1.8–5.31) was expected, as this value depends on the nonlinear relationship between the recorded rainfall event and the observed runoff hydrograph of that particular event. For example, while the Phi value in a storm no. 2 was 4.23 and the corresponding rainfall excess was 0.167 mm, in a storm no. 1 (plot (a) of Fig. 7) the Phi value was 1.86 while the corresponding rainfall excess was 0.24 mm.

The simulated hydrographs by this approach are shown in Fig. 7 in red. Good agreements in the values of $Q_v$, $Q_p$, and $T_p$ were achieved. Although there was an underestimation in some simulated hydrograph parameters and an overestimation in others, results obtained by this method are much better than those obtained by LIA and slightly better than those obtained by HIM. The maximum difference between observed and simulated $Q_p$ was 1.03%. This low percentage indicates a perfect match between observed and simulated values and is also comparable and competitive with many results in the literature. For example, Majidi and Shahedi [37] obtained a difference of 9.1% in $Q_p$ using HEC-HMS with the Green–Ampt method. Moreover, a perfect match was obtained in $Q_v$ in all storms with $R^2 = 1$.

To show differences in computed and observed hydrograph parameters, the values of observed and simulated $Q_p$, $Q_v$, and $T_p$ are plotted in 1:1 graph for all storms as shown in Fig. 8. Each plot in Fig. 8 contains 12 scatter points corresponding to four storms simulated by the two approaches.

Table 2
Computed Phi index values for different storms at runoff station

| Storm no. | Rainfall excess (mm) | Phi value |
|---|---|---|
| 1 | 0.24 | 1.86 |
| 2 | 0.167 | 4.23 |
| 3 | 2.46 | 5.31 |
| 4 | 0.48 | 2.43 |

A perfect match between observed and simulated $Q_p$ and $Q_v$ was found in all storms in the case of ERAs. In both HIM and PIM methods, all points fall approximately on 45° line with the $R^2$ value of approximately 1 (Figs. 8(a) and (b)). Simulated flow volumes, on the other hand, were not in a good agreement with the observed values under the LIA approach as shown in Fig. 8(b) (black circles). There was an overestimation in $Q_v$ by this approach in all simulated storms. The worst match between observed and simulated in all of the approaches was found in $T_p$ (as shown in Fig. 8(c)). The maximum deviation from the 45° line was obtained by the results of LIA where all the simulated storms overestimated the observed values. Although ERA by HIM and PIM methods slightly overestimated $T_p$ with an $R^2$ value equal to 0.81 and 0.72, a slight overestimation was found with ERAs HIM and PIM and $R^2$ value equal to 0.78 and 0.72, respectively, thereby indicating a good and acceptable match. In general, all simulations overestimated the $T_p$ but the ERA performed better than LIA. This result might suggest a spatial variability in the rainfall distribution.

Table 3 shows that the total and average absolute residuals are high in all storms simulated by LIA and ERA. Those simulated by ERAs via HIM and PIM produced minimum absolute residuals, thereby showing a good performance by these approaches with preference to Phi index approach.

Sensitivity analysis on basin characteristics considered in the model revealed that the peak flow is directly proportional to the CN and inversely proportional to the $I_a$. For example, in storm no. 1 with CN of 90 and initial abstraction of 0.385 mm, the corresponding simulated peak was 6.13 m³/s. If we reduce the CN to 80 about 11% and keep $I_a$ = 0.385 constant, the resultant peak flow will be reduced to 5.54 m³/s about 9 %. Similarly, if we increase the $I_a$ to 1 mm about 61% and keep CN = 90 constant, the resultant peak flow will be reduced to 5.77 m³/s about 5.8%. However, time lag effect is quite different, as it causes peak flow to flatten and spread over a longer duration. For example, if we keep CN = 90 and $I_a$ = 0.385 mm constant in the storm no. 1 and change only the lag time ($T_L$ = 536–600 min), the resultant peak flow will be attenuated from $Q_p$ = 6.11–5.55 m³/s (9% reduction in $Q_p$). However, with ERAs, good matches of $Q_p$, $Q_v$, and $T_p$ between observed and simulated hydrographs were obtained. Therefore, it is concluded that rainfall–runoff analyses in arid regions such as Wadi Al-Lith are better simulated by the proposed ERAs.

Excluding LIA results, simulated hydrographs by HIM and PIM indicated that approximately more than 80% of rainwater of the studied storms was distributed among initial abstraction, evaporation, and infiltration. Constant initial abstraction is widely used assumption and applied in many hydrological studies [38,39]. Initial abstraction ratio ranging from 0.0 to 0.2 was reported in the literature [40,41].

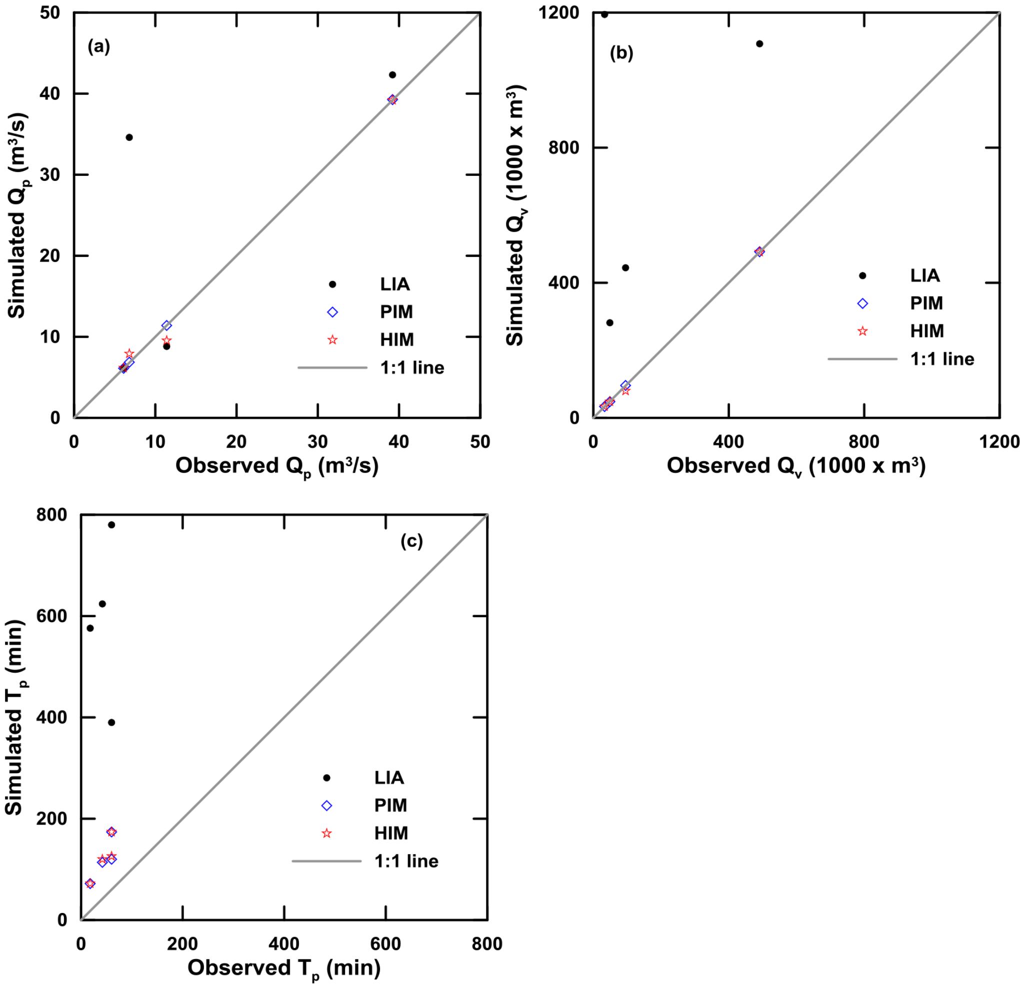


Fig. 8. (a) $Q_p$, (b) $Q_v$ and (c) $T_p$ model parameters performance, plotted on 1:1 graph for the three simulation methods.

Table 3
Residuals of $Q_p$ and $Q_v$ for the LIA and ERA approaches

| Property | Storm no. | LIA | HIM | PIM |
|---|---|---|---|---|
| Average absolute residuals ($m^3/s$) | 1 | 1.92 | 0.23 | 0.23 |
| | 2 | 17.82 | 0.29 | 0.36 |
| | 3 | 3.37 | 1.55 | 0.43 |
| | 4 | 13.45 | 4.63 | 4.45 |
| Total residuals (1,000 $m^3$) | 1 | 229.7 | –0.7 | –0.7 |
| | 2 | 840.2 | 0.2 | 0.2 |
| | 3 | 284.9 | –18.3 | 0.8 |
| | 4 | 532.8 | –5.8 | –3.9 |

Results from relevant studies showed that the average ratio of initial abstraction to maximum potential retention in arid areas is about 5% [42]. On the other hand, evapotranspiration during rainfall events is negligible compared with the total rainfall amount [43–45], the main reason for that is the short duration of the rainfall event. However, evapotranspiration becomes significant after rainfall ceases. In this context, the major amount of rainfall is devoted to the infiltration process. About 55%–70% of rainwater infiltrates through the soil profile and recharges the underlined groundwater reservoir, consequently becomes a major source of water in the region. The quality of this water is good enough for many purposes including agriculture, industry, and even drinking purposes. However, a minimum treatment is required for drinking water purposes. Commonly, filtration and disinfection of well water are widely applied [46].

## 4. Conclusions

Spatial distribution of rainfall and antecedent moisture condition are two important phenomena that are not effectively manipulated in the SCS method; therefore, overestimation and underestimation of peak flow, time to peak, and volume of flow were simulated. The rainfall–runoff relationship of Wadi Al-Lith is highly nonlinear. Although all selected and simulated storms occurred within 4 months, they produced a wide range of runoff coefficients (1%–21%) which indicate a complex flow system. LIA performance was poor in simulating runoff hydrographs in all storms. Therefore, caution must be taken when considering the application of this approach to similar case studies. Its two main drawbacks were the generation of runoff with no lag time between rainfall and runoff, and the ineffective representation of flow mass conservation. On the other hand, the proposed effective rainfall approaches simulated runoff hydrographs efficiently with results that are comparable with many which have been reported in the literature. Phi index performed better than Horton's infiltration approach; however, both can be recommended for prediction of runoff hydrographs of arid or semi-arid watersheds such as Wadi Al-Lith. Among all hydrograph parameters, the two effective rainfall approaches predict peak flow more accurately followed by time to peak. The sensitivity analysis revealed that the peak flow is directly proportional to the CN and inversely proportional to the initial abstraction. The simulation results added a valuable piece of information about the groundwater share from total rainwater. About 55%–70% of rainwater recharges the underlined groundwater reservoir and becomes a major source of clean water in the region.

## Acknowledgments

This project was funded by the National Plan for Science, Technology and Innovation (MAARIFAH) – King Abdulaziz City for Science and Technology – the Kingdom of Saudi Arabia – award number (11-WAT1999-03). The authors also thank Science and Technology Unit, King Abdulaziz University for technical support.

## Symbols

| | | |
|---|---|---|
| DEM | — | Digital elevation model |
| CN | — | Curve number |
| ERA | — | Excess rainfall approach |
| $f_p$ | — | Infiltration capacity |
| $f_c$ | — | Final or equilibrium capacity |
| $f_0$ | — | Initial infiltration capacity |
| HEC-HMS | — | Hydrologic Engineering Center's Hydraulic Modeling System (US Army Corps of Engineers) |
| IHACRES | — | Identification of unit hydrographs and component flows from rainfall, evaporation and streamflow data |
| $I_a$ | — | The initial abstraction |
| $k$ | — | Constant that represents the rate of decrease in $f$ capacity |
| LIA | — | Losses incorporation approach |
| $P$ | — | Accumulated rainfall depth |
| $P_e$ | — | Accumulated precipitation excess |
| PIM | — | Phi index method |
| $P_n$ | — | Observed rainfall |
| $\phi$ | — | Phi index |
| $Q_p$ | — | Peak flow |
| $Q_v$ | — | Runoff volume |
| $R^2$ | — | Regression coefficient |
| $R_d$ | — | Direct runoff depth |
| $S$ | — | Potential maximum retention |
| SCS | — | Soil conservation service |
| $t$ | — | Time |
| $T_L$ | — | Lag time |
| $T_p$ | — | Time to peak flow |

## References


[1] H. Wheater, S. Sorooshian, K.D. Sharma, Hydrological Modelling in Arid and Semi-Arid Areas, Cambridge University Press, UK, 2007.

[2] M.N. French, W.F. Krajewski, R.R. Cuykendall, Rainfall forecasting in space and time using a neural network, J. Hydrol., 137 (1992) 1–31.

[3] A.Y. Shamseldin, Application of a neural network technique to rainfall-runoff modelling, J. Hydrol., 199 (1997) 272–294.

[4] K. Beven, Infiltration excess at the Horton Hydrology Laboratory (or not?), J. Hydrol., 293 (2004) 219–234.

[5] J. Merz, P.M. Dangol, M.P. Dhakal, B.S. Dongol, G. Nakarmi, R. Weingartner, Rainfall-runoff events in a middle mountain catchment of Nepal, J. Hydrol., 331 (2006) 446–458.

[6] P. Brunner, J. Doherty, C.T. Simmons, Uncertainty assessment and implications for data acquisition in support of integrated hydrologic models, Water Resour. Res., 48 (2012) p. W07513, http://dx.doi.org/10.1029/2011WR011342.

[7] M.-J. Shin, J.H. Guillaume, B.F. Croke, A.J. Jakeman, A review of foundational methods for checking the structural identifiability of models: results for rainfall-runoff, J. Hydrol., 520 (2015) 1–16.

[8] M. Anderson, Z.-Q. Chen, M. Kavvas, A. Feldman, Coupling HEC-HMS with atmospheric models for prediction of watershed runoff, J. Hydrol. Eng., 7 (2002) 312–318.

[9] V. Gardiner, Drainage Basin Morphometry, A. Goudie, Ed., Geomorphological Techniques, Unwin Hyman, London, 1990, pp. 71–81.

[10] P.C. Patton, Drainage Basin Morphometry and Floods, Flood Geomorphology, John Wiley & Sons, New York, 1988, pp. 51–64.

[11] L. Olang, J. Fürst, Effects of land cover change on flood peak discharges and runoff volumes: model estimates for the Nyando River Basin, Kenya, Hydrol. Proc., 25 (2011) 80–89.

[12] A. Biswas, D. Das Majumdar, S. Banerjee, Morphometry governs the dynamics of a drainage basin: analysis and implications, Geogr. J., 2014 (2014), Article ID 927176, 14 pages http://dx.doi.org/10.1155/2014/927176.

[13] I.A. Abboud, R.A. Nofal, Morphometric analysis of wadi Khumal basin, western coast of Saudi Arabia, using remote sensing and GIS techniques, J. Afr. Earth Sci., 126 (2017) 58–74.

[14] M. Sangati, M. Borga, Influence of rainfall spatial resolution on flash flood modelling, Nat. Hazard Earth Syst. Sci., 9 (2009) 575–584.

[15] I. Abustan, A.H. Sulaiman, N. Abdul Wahid, F. Baharudin, Determination of Rainfall-Runoff Characteristics in an Urban Area: Sungai Kerayong Catchment, Kuala Lumpur, 2008.

[16] E. Bournaski, R. Iliev, L. Kirilov, HEC-HMS modelling of rainstorm in a catchment. The Mesta case study, C.R. Acad. Bulgare Sci., 62 (2009) 1141–1146.

[17] M. Al-Ahmadi, A. El-Fiky, Hydrogeochemical evaluation of shallow alluvial aquifer of Wadi Marwani, western Saudi Arabia, J. King Saud Univ. Sci., 21 (2009) 179–190.

[18] M. Knebl, Z.-L. Yang, K. Hutchison, D. Maidment, Regional scale flood modeling using NEXRAD rainfall, GIS, and HEC-HMS/RAS: a case study for the San Antonio River Basin Summer 2002 storm event, J. Environ. Manage., 75 (2005) 325–336.

[19] Z. Yusop, C. Chan, A. Katimon, Runoff characteristics and application of HEC-HMS for modelling stormflow hydrograph in an oil palm catchment, Water Sci. Technol., 56 (2007) 41–48.

[20] E. Abushandi, B. Merkel, Modelling rainfall runoff relations using HEC-HMS and IHACRES for a single rain event in an arid region of Jordan, Water Resour. Manage., 27 (2013) 2391–2409.

[21] J. Du, L. Qian, H. Rui, T. Zuo, D. Zheng, Y. Xu, C.-Y. Xu, Assessing the effects of urbanization on annual runoff and flood events using an integrated hydrological modeling system for Qinhuai River basin, China, J. Hydrol., 464 (2012) 127–139.

[22] S. Shadeed, M. Almasri, Application of GIS-based SCS-CN method in West Bank catchments, Palestine, Water Sci. Eng., 3 (2010) 1–13.

[23] F. Radmanesh, J.P. Hemat, A. Behnia, A. Khond, B.A. Mohamad, Calibration and Assessment of HEC-HMS Model in Roodzard Watershed, 17th International Conference of River Engineering, University of Shahid Chamran, Ahva, 2006.
[24] T. Kafle, M. Hazarika, S. Karki, R. Shrestha, S. Sharma, L. Samarakoon, Basin Scale Rainfall-Runoff Modelling for Flood Forecasts, Proc. 5th Annual Mekong Flood Forum, Ho Chi Minh City, Vietnam, 2007, pp. 17–18.
[25] F.S. Al-Ahmadi, Rainfall-Runoff Modeling in Arid Regions Using Geographic Information Systems and Remote Sensing: Case Study; Western Region of Saudi Arabia, King Abdulaziz University Jeddah, 2005.
[26] D.G. Hadley, R.J. Fleck, Reconnaissance Geology of the Al Lith Quadrangle, Sheet 20/40 C, Kingdom of Saudi Arabia, US Geological Survey, 1979.
[27] S. Bajabaa, M. Masoud, N. Al-Amri, Flash flood hazard mapping based on quantitative hydrology, geomorphology and GIS techniques (case study of Wadi Al Lith, Saudi Arabia), Arab. J. Geosci., 7 (2014) 2469–2481.
[28] D. Moore, Representative Basins Study for Wadis: Yiba, Habawnah, Tabalah, Liyyah and Lith, Final Report by Dames & Moore, Saudi Arabia to Ministry of Agriculture and Water, Riyadh, 1988.
[29] W. Scharffenberg, A. Feldman, Joint Conference on Water Resource Engineering and Water Resources Planning and Management, Minneapolis, MN, USA, 2000.
[30] A.D. Feldman, Hydrologic Modeling System HEC-HMS: Technical Reference Manual, US Army Corps of Engineers, Hydrologic Engineering Center, 2000.
[31] R.E. Horton, An approach toward a physical interpretation of infiltration-capacity, Soil Sci. Soc. Am. J., 5 (1941) 399–417.
[32] R.K. Linsley, M.A. Kohler, J.L.H. Paulhus, Applied Hydrology, McGraw-Hill, New York, 1949.
[33] M.N. Allam, K.S. Balkhair, Case study evaluation of the geomorphologic instantaneous unit hydrograph, Water Resour. Manage., 1 (1987) 267–291.
[34] R. Meenu, S. Rehana, P. Mujumdar, Assessment of hydrologic impacts of climate change in Tunga–Bhadra river basin, India with HEC-HMS and SDSM, Hydrol. Processes., 27 (2013) 1572–1589.
[35] G.M. Reza, Evaluation of flood mitigation alternatives using hydrological modeling, J. Appl. Sci. Environ. Manage., 11 (2007) 113–117.
[36] H. Jin, R. Liang, Y. Wang, P. Tumula, Flood-runoff in semi-arid and sub-humid regions, a case study: a simulation of Jianghe watershed in Northern China, Water, 7 (2015) 5155–5172.
[37] A. Majidi, K. Shahedi, Simulation of rainfall-runoff process using Green-Ampt Method and HEC-HMS model (case study: Abnama Watershed, Iran), Int. J. Hydraul. Eng., 1 (2012) 5–9.
[38] W.H. Asquith, M.C. Roussel, An Initial-Abstraction, Constant-Loss Model for Unit Hydrograph Modeling for Applicable Watersheds in Texas, US Geological Survey, 2007.
[39] L.W. Mays, Water Resources Engineering, John Wiley & Sons, NY, USA, 2010.
[40] E. Baltas, N. Dervos, M. Mimikou, Determination of the SCS initial abstraction ratio in an experimental watershed in Greece, Hydrol. Earth Syst. Sci., 11 (2007) 1825–1829.
[41] R.H. Hawkins, T.J. Ward, D.E. Woodward, J.A. Van Mullem, Continuing Evolution of Rainfall-Runoff and the Curve Number Precedent, Proc. 2nd Joint Federal Interagency Conference, 2010.
[42] Z.-H. Shi, L.-D. Chen, N.-F. Fang, D.-F. Qin, C.-F. Cai, Research on the SCS-CN initial abstraction ratio using rainfall-runoff event analysis in the Three Gorges Area, China, CATENA, 77 (2009) 1–7.
[43] J. Marsalek, C. Maksimovic, E. Zeman, R. Price, Hydroinformatics Tools for Planning, Design, Operation and Rehabilitation of Sewer Systems, Springer Science & Business Media, Netherlands, 2013.
[44] D.E. Overton, M.E. Meadows, Stormwater Modeling, Academic Press, New York, 1976.
[45] C.W. Rose, An Introduction to the Environmental Physics of Soil, Water and Watersheds, Cambridge University Press, UK, 2004.
[46] J.K. Edzwald, Water Quality and Treatment a Handbook on Drinking Water, McGraw Hill, New York, USA, 2010.